

Effects of Two-Step Sintering on the Microstructure of Si_3N_4

Jow-Lay Huang,^a Li-Mei Din,^a Horng-Hwa Lu^a & Wen-Hu Chan^b

^aDepartment of Materials Science and Engineering, National Cheng Kung University, Tainan, Taiwan

^bDepartment of Mechanical Engineering, Chinese Military Academy, Taiwan

(Received 19 December 1994; accepted 1 March 1995)

Abstract: The microstructure of two-step sintered silicon nitride was studied. An investigation was undertaken concentrating on the effects of microstructure developed after the initial stage sintering on the grain size distribution and aspect ratio in β -grains during the final stage of sintering.

Experimental results indicated that the grain size increased, grain size distribution became wider, and more volume of large grains was developed with increase of presintering temperature and time. The aspect ratio could increase or decrease with presintering temperature, depending on the duration of the initial stage sintering.

1 INTRODUCTION

Silicon nitride has attracted considerable attention over the past two decades owing to its excellent mechanical, chemical and thermal properties at room and elevated temperatures.

The microstructural development in silicon nitride, especially the grain size distribution and aspect ratio developed during sintering, has had prominent effects on the R-curve behaviour,^{1–6} fracture toughness and fracture mechanisms^{4,5,9,10} and other mechanical properties.^{7,8} Significant success has been achieved with the so-called ‘*in-situ*-reinforcement’ technique. This approach would be highly desirable since many problems associated with the use of secondary toughening phases could be avoided.

Most investigations concerned with parameters for the microstructural development of silicon nitride have emphasized the role of the characteristics of powders, i.e. the particle size distribution, amount and morphology of the β -particles.^{11,12} This study adopted a different approach. In this work, the development of a needle-like micro-structure in Si_3N_4 is studied via a two-step sintering process. Particular emphasis is placed on the effects of microstructural development after the initial stage of sintering toward the development of grain size distribution and aspect ratio of β -grains during the final stage of sintering.

2 EXPERIMENTAL PROCEDURES

2.1 Powder mixing

Silicon nitride powder (UBE Corp., SN-E10) of size $0.2\ \mu\text{m}$ was mixed with yttria (6 wt%, Moly-corp, Grade 5603) and alumina (2 wt%, Alcoa, Grade 16SG) in a polyethylene bottle with high purity alumina balls ($\Phi = 10\ \text{mm}$) and ethanol for 24 h. The weight ratio of charge to balls was 1:8. The slurry was ultrasonically dispersed for 3 min and then dried in a rotating evaporator. Dried powders were ground in an alumina mortar and pestle, passed through a 100-mesh screen and cold isostatically pressed into bars at 680 MPa.

2.2 Two-step sintering

Samples were embedded in a powder bed consisting of 50% BN and 50% Si_3N_4 (with sintering additives) by mass in a graphite crucible to minimize the vaporization of liquid phase and decomposition of silicon nitride during sintering.

Samples were first sintered at 1550°C, 1600°C and 1650°C for 1 or 3 h at 0.1 MPa nitrogen atmosphere in a graphite furnace for controlling the nucleation and growth of the β -phase. They were subsequently sintered in a graphite furnace (Fuji Dempa High Myliti 5000) at 1900°C for 3 h at 1 MPa of nitrogen.

2.3 Characterization

2.3.1 Density

The density was measured by water displacement technique. The relative density was calculated from the theoretical density of each constituent and its content.

2.3.2 Phase identification

An X-ray diffractometer (Rigaku D/Max-IIIB) with a Cu target and Ni filter was used to determine the phase contents. Samples were scanned from 20° to 80° with a scanning rate of 4°/min, and from 30° to 40° with a scanning rate of 0.5°/min, respectively. The technique derived by Gazzara¹³ was used for determining the phase contents in Si₃N₄.

2.3.3 Microstructural analysis

Samples were polished to 1 µm, chemically etched in NaOH melt at 350°C for 1–1.5 min and coated with Au for STEM (Scanning Transmission Electron Microscope, Hitachi H-700H) analysis. Grain size and aspect ratio were measured by image analyzer associated with OPTIMAS (software name, Bioscan Inc., Edmonds, Washington USA), and calculated following the statistical derivation by Woetting *et al.*¹⁴ The 'true' aspect ratio was obtained from the frequency distribution of the aspect ratios for approximately 2500 grains which were visible in a microsection, subsequently selecting the value as a_{95} . In other words, 5% of all visible grains exhibited a higher aspect ratio and 95% demonstrated a lower aspect ratio than the 'true' aspect ratio.

Since it was anticipated that the small volume of large grains had prominent effects on the fracture mechanisms, e.g. crack bridging and deflection,^{4,15} the sizes of the large grains were also determined. On each five fields of SEM photographs (1000x) of fractured surfaces of a specimen, 10 'coarse' acicular grains were selected. The average value of the largest 10 out of 50 measurements was defined as the average size of large grains.

3 RESULTS AND DISCUSSION

3.1 Initial-stage sintering

3.1.1 Shrinkage, density and phases

Table 1 summarizes the linear shrinkage, relative density and β -phase content of Si₃N₄ after being presintered at 1550°C, 1600°C and 1650°C for 1 or 3 h. These experimental results indicated that the linear shrinkage, density and β -phase content increased with presintering temperature and time.

The shrinkage in the initial stage in a SiO₂–

Table 1. Relative density, linear shrinkage and β -phase content of Si₃N₄ after presintering at 1550°C, 1600°C and 1650°C for 1 or 3 h

Presintering temperature (°C)	1550		1600		1650	
Time (h)	1	3	1	3	1	3
Relative density (%)	89.0	90.1	89.5	—	90.5	92.4
Linear shrinkage (%)	18.0	19.5	19.5	—	20.3	21.4
β -phase (%)	30.7	71.1	89.4	—	100.0	100.0

Al₂O₃–Y₂O₃ system, which was attributed to particle rearrangement, was reported to occur at 1350°C, i.e. the eutectic formation temperature.¹⁶ The relatively higher presintering temperatures used in this study produced a considerable shrinkage, high density and phase conversion as revealed in Table 1. A shrinkage of 21.4% and relative density of 92.4% were obtained in samples presintered at 1650°C for 3 h.

Samples presintered at 1600°C for 1 h apparently had a slightly lower density than samples presintered at 1550°C for 3 h although more α -phase was converted (Table 1). This observation suggested that the α – β transition does not directly relate to the densification.¹⁷

Prokesova reported that the α – β transformation of Si₃N₄ during liquid phase sintering was primarily controlled by the diffusion through the liquid in the case of Y₃Al₅O₁₂ additives.¹⁸ This was probably why more α – β phase conversion was observed with the increase of presintering temperature and time.

3.1.2 Microstructure

Figure 1 shows the SEM micrographs of silicon nitride after being presintered at 1550°C, 1600°C and 1650°C for 1 or 3 h. Equiaxed grains with narrow size distribution and porous structure were observed in samples presintered at relatively low temperatures. Rod-like grains with high aspect ratios were developed and the grain size distribution became quite wide, however, with presintering temperature and time.

3.2 Final-stage sintering

3.2.1 Density, shrinkage and phase content

The presintered samples were subsequently sintered at 1900°C for 3 h. The measured density, linear shrinkage and β -phase content are summarized in Table 2. These results indicated that both the density and shrinkage of two-step sintered samples increased with the presintering temperature

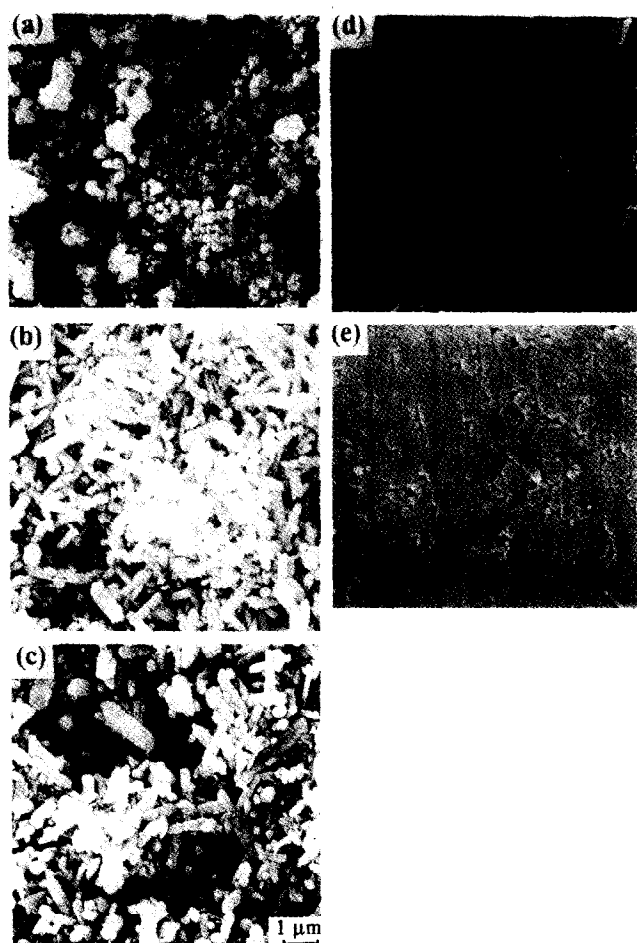


Fig. 1. SEM micrographs of silicon nitride after being presintered at (a) 1550°C, 1 h, (b) 1600°C, 1 h, (c) 1650°C, 1 h, (d) 1550°C, 3 h and (e) 1650°C, 3 h.

and time, and were always higher than those of one-step sintered samples.

The lower viscosity of the glass phase produced by heat treatment above the glass transition temperature leads to an increase in the volume of pores near the mean pore radius and a reduction in the volume of large pores through increased flow which allows for increased rearrangement as previously reported.¹⁸ The lower viscosity which appeared at higher presintering temperatures used in this study could therefore improve the uniformity of pore

Table 2. Relative density, linear shrinkage and β -phase content of Si_3N_4 after sintering at 1900°C for 3 h. Some samples were presintered at 1550°C, 1600°C and 1650°C for 1 or 3 h

Presintering temperature (°C)	None (one-step sintering)	1550		1600		1650	
Presintering time (h)	0	1	3	1	3	1	3
Relative density (%)	96.8	97.2	97.6	97.8	—	98.4	98.6
Linear shrinkage (%)	19.9	20.4	20.8	20.5	—	22	22.6
β -phase (%)	100	100	100	100	—	100	100

size distribution which persists through the densification process in the final-stage sintering, thereby resulting in higher shrinkage and density.^{19,20}

The full conversion of α into β -phase was noticed after being sintered at 1900°C for 3 h (Table 2).

3.2.2 Grain size

The frequency distributions of grain size of two-step sintered Si_3N_4 with presintering times of 1 and 3 h were separately measured and compared with that of one-step sintered samples (Fig. 2a, b). These figures revealed that the grain size at maximum frequency had a tendency to increase; in addition, larger grains were observed as the presintering temperature and time were increased. Furthermore, the two-step sintered Si_3N_4 consistently had a larger grain size at maximum frequency and more volume of large grains than one-step sintered Si_3N_4 .

Since the grain size distributions in Fig. 2 were not symmetrical, the average grain size was further determined by taking the mean size at half of maximum frequency and is illustrated in Fig. 3. This figure clearly indicated a trend of grain size increase with presintering temperature and time.

The size distributions of the grains (Fig. 2a, b) were further normalized by the average grain size and expressed as shown in Fig. 4a, b. These figures revealed that the distribution of grain sizes became wider with presintering temperature and time.

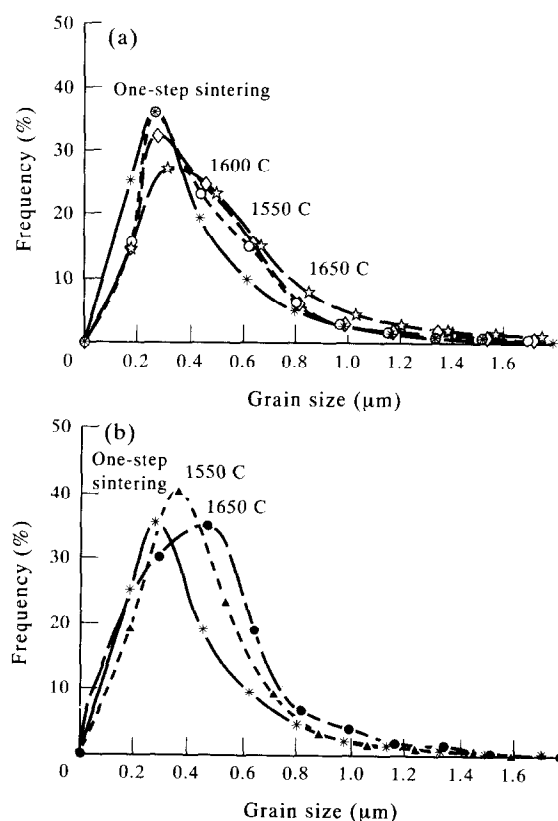


Fig. 2. Grain size distribution of silicon nitride sintered at 1900°C for 3 h. Samples presintered at 1550°C, 1600°C and 1650°C for 1 h (a) or 3 h (b).

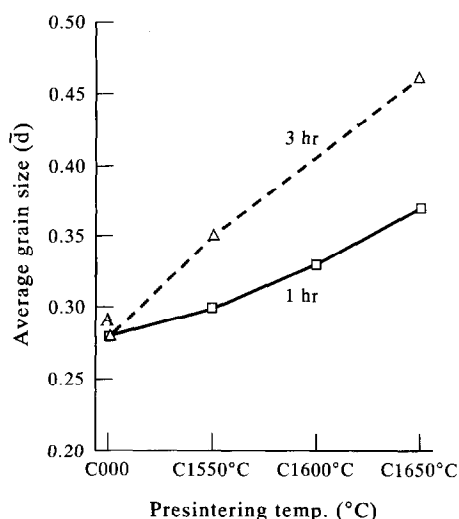


Fig. 3. Average grain size of silicon nitride sintered at 1900°C for 3 h. Samples presintered at 1550°C, 1600°C and 1650°C. Point A indicates the grain size of one-step sintered samples.

Parameters controlling the size and aspect ratio of elongated Si_3N_4 grains were earlier discussed. Those factors for controlling the microstructural development of Si_3N_4 include sintering additives,^{21–24} sintering conditions,²⁵ and the amount and size distribution of $\beta\text{-Si}_3\text{N}_4$ particles in the starting powder.^{12,26}

It was previously reported that β -particles could act as nuclei if they have a size greater than the

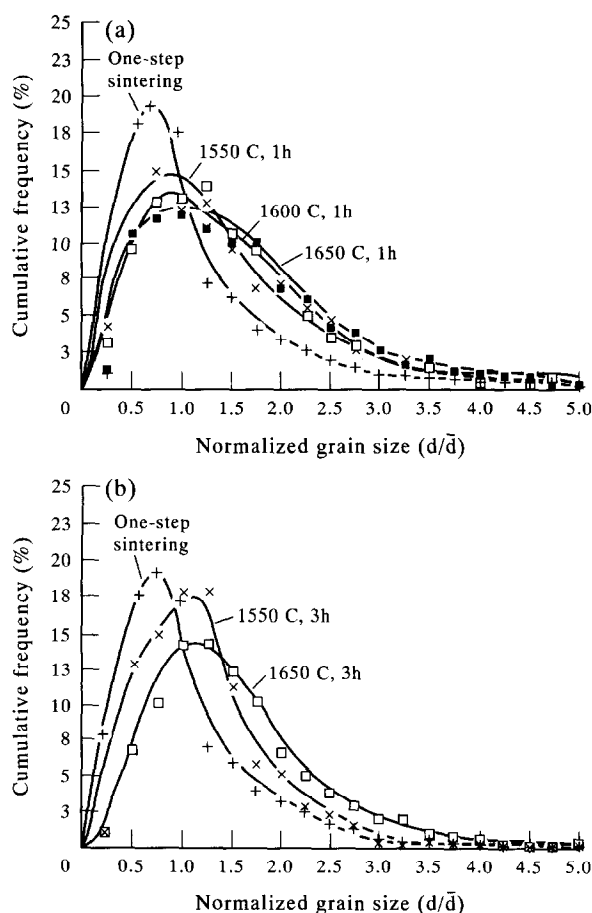


Fig. 4. Normalized grain size distribution of silicon nitride sintered at 1900°C for 3 h. Some samples presintered at 1550°C, 1600°C and 1650°C for 1 h (a) or 3 h (b).

mean size of the β -grains resulting from the α - β conversion at the beginning of the solution-precipitation stage. Otherwise, they become dissolved in the liquid phase due to the energy potential difference between small and large-sized grains.¹¹ Dressler²⁷ and Becher²⁸ also proposed that the number of large grains in sintered Si_3N_4 depends on the initial β -particle size distribution of the starting powder.

The relatively larger grain size and wider grain size distribution in two-step sintered Si_3N_4 possibly resulted from the relatively larger grains, and broader distribution of grain sizes developed after the initial stage sintering (Fig. 1). The inhomogeneous microstructure developed after presintering probably became more pronounced through the mechanisms of solution-diffusion-precipitation and pore coalescence during the final stage of sintering.

3.2.3 Large grains

The average sizes of large grains are also plotted in Fig. 5 as a function of presintering temperature. Similarly to Fig. 3, the size of large grains also increased with presintering temperature and time.

Woetting¹¹ reported that only a small number of coarse grains with needle-like morphology and suitable crystallographic orientation were favourable for the formation of large grains. The growth of anisotropical grains is not directly related to the phase transformation but to the large difference in solubility between grains of different grain size as also reported by Mitomo.²⁹

The wide distribution in grain sizes, inhomogeneous and distinctive microstructure developed in β -grains after presintering were also possibly responsible for the development of some extremely large grains during the final-stage sintering.

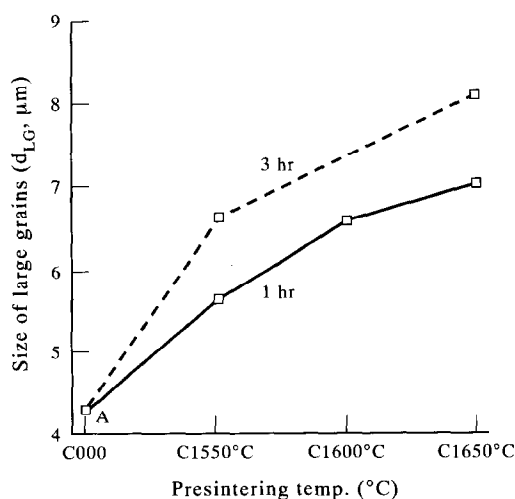


Fig. 5. Average diameter of large grains of silicon nitride sintered at 1900°C for 3 h. Some samples presintered at 1550°C, 1600°C and 1650°C. Point A indicates the large grain size of one-step sintered samples.

3.2.4 Aspect ratio

A typical cumulative frequency distribution of aspect ratio of one-step sintered Si_3N_4 and samples presintered at 1550°C, 1600°C, 1650°C for 1 h before final-stage sintering is illustrated in Fig. 6. The 'true' aspect ratio, a_{95} , calculated from Fig. 6 following Woetting's derivation,¹⁴ is also plotted in Fig. 7 as a function of presintering temperature. Point A indicates one-step sintered samples. This figure revealed that the aspect ratio continuously increased, but not linearly, with presintering temperature. A maximum aspect ratio of 8 was obtained in samples presintered at 1650°C for 1 h.

The observation of samples exhibiting an increased aspect ratio with presintering temperature was probably related to a model proposed by Koessel *et al.*³⁰ They reported that the energetically more favourable surface nucleation on the basal plane would probably account for the higher growth rate in comparison to the prism plane.

The aspect ratio of Si_3N_4 presintered for longer

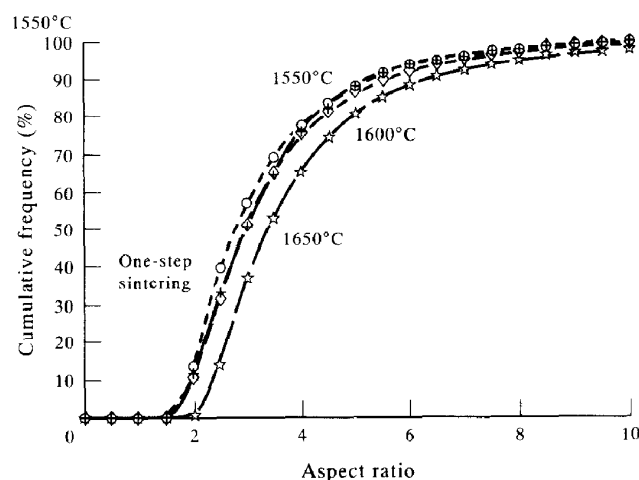


Fig. 6. Cumulative frequency distribution of the aspect ratio of silicon nitride sintered at 1900°C for 3 h. Some samples presintered at 1550°C, 1600°C and 1650°C for 1 h.

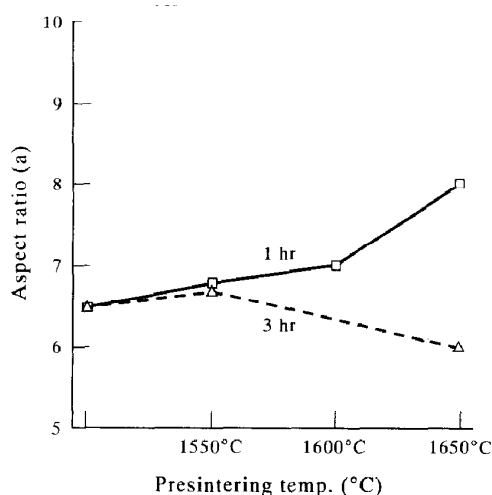


Fig. 7. Aspect ratio of silicon nitride sintered at 1900°C for 3 h. Some samples presintered at 1550°C, 1600°C and 1650°C. Point A indicates the aspect ratio of one-step sintered samples.

than 3 h before final-stage sintering was also calculated and plotted in Fig. 7. In contrast to samples presintered for only 1 h, the aspect ratio actually decreased with presintering temperature. As the presintering temperature continued increasing, it became substantially lower than that of samples presintered for 1 h.

The average grain length measured in samples after the final-stage sintering is plotted in Fig. 8 as a function of presintering temperature. The grain lengths noticeably increased with presintering temperature despite their presintering duration. This was particularly interesting for samples presintered for 3 h since their aspect ratio actually decreased with presintering temperature.

Petzow and Hoffman¹² used model experiments on isolated Si_3N_4 crystals embedded in super-saturated Si-Al-O-N glasses to investigate the development of microstructure during the α - β transformation and the Ostwald-ripening stage. The development of mean aspect ratio was found to exhibit a strong increase during the α - β transformation and then remained constant or even reduced during the subsequent Ostwald-ripening stage depending on the treatment temperature.

The observation of a decrease in aspect ratio with presintering temperature in samples presintered for a long duration could probably be ascribed to the following reasons: (1) For longer isothermal times, the microstructure could reach thermodynamic equilibrium, and a small driving force depending only on the differences in grain size³¹ caused the slow grain growth. (2) Small β grains with high aspect ratio were probably redissolved. (3) The growth of β -needles was hindered by the surrounding grains.¹²

Results obtained in Fig. 7 are also supported by the observations from SEM micrographs as shown

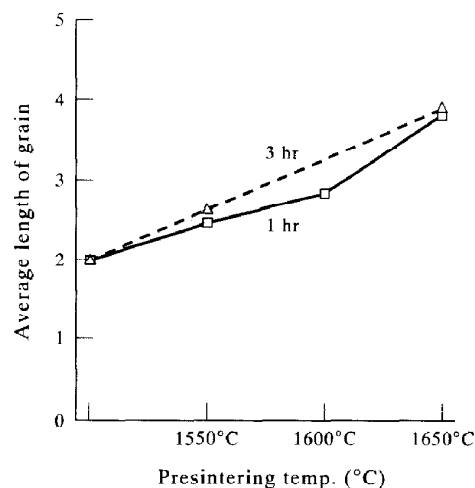


Fig. 8. Average grain length of silicon nitride sintered at 1900°C for 3 h. Some samples presintered at 1550°C, 1600°C and 1650°C. Point A indicates the grain length of one-step sintered samples.

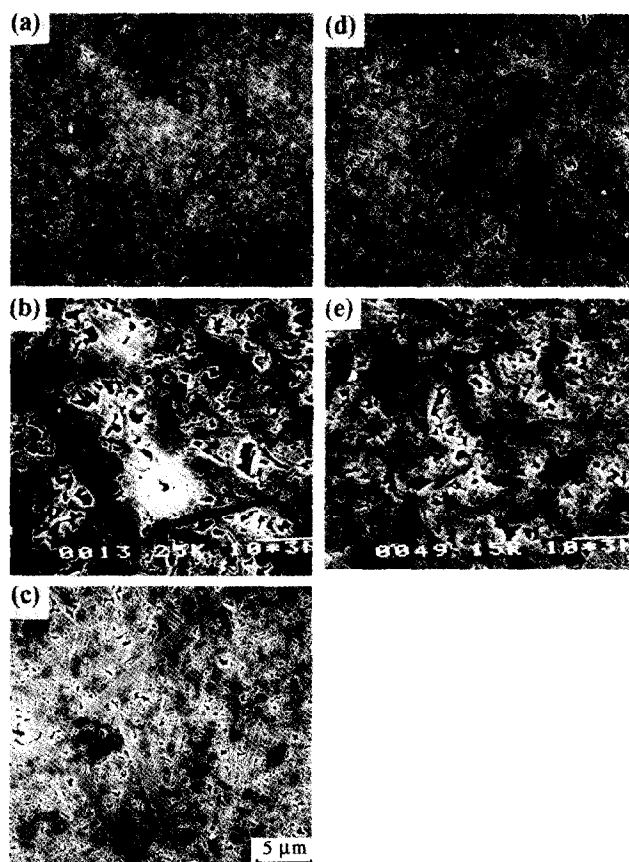


Fig. 9. SEM micrographs of silicon nitride sintered at 1900°C for 3 h. Samples were presintered at (a) 1550°C 1 h, (b) 1600°C 1 h, (c) 1650°C 1 h, (d) 1550°C 3 h and (e) 1650°C 3 h.

in Fig. 9. In order to obtain grains with a high aspect ratio, the selection of high presintering temperature is apparently quite essential, but not for a long period. Long presintering time after the α - β conversion generally causes the formation of equiaxed grains and decreases the aspect ratio.

However, no evidence suggested that the amount of β -phase before the final stage sintering played any role in the development of microstructure.

4 CONCLUSIONS

The following conclusions could be drawn on the basis of the above discussion:

(1) The linear shrinkage, density and β -phase increased, grain size distribution became wider, grain size increased, and a greater volume of large grains was developed with the increase of presintering temperature and time. However, the aspect ratio decreased with presintering temperature for samples presintered for 3 h.

(2) The microstructure developed after the initial-stage sintering exerted direct and quite prominent effects on the final microstructure developed in two-step sintered Si_3N_4 .

ACKNOWLEDGEMENT

The authors would like to thank the National Science Council of Taiwan for its financial support under the contract No. NSC 82-0405-E-006-236.

REFERENCES

1. TANI, E., UMEBAYASHI, S., KOBAYASHI, K. & NISHIJIMA, M., *Am. Ceram. Soc. Bull.*, **65** (1986) 1311-15.
2. MITOMO, M., *MRS Internat. Mtg on Adv. Mats*, 5. Mater. Res. Soc. 1989, p. 69.
3. TAJIMA, Y., URASHIMA, K., WATANABE, M. & MATSUO, Y., *Ceram. Transaction 1/Proc. 1st Internat. Conf. Cer. Powder Proc. Sci.*, Orlando, 1987.
4. BECHER, P., *J. Am. Ceram. Soc.*, **74** (1991) 255.
5. LI, C. W. & YAMANIS, J., *Ceram. Eng. Sci. Proc.*, **10** (1989) 632-45.
6. OKADA, A. & HIROSAKI, N., *J. Mater. Sci.*, **25** (1989) 1656.
7. SALGANIK, R. L., *Mech. Solids*, **8** (1973) 135.
8. ZIMMERMAN, R. W., *Int. J. Rock Mech. Min. Sci., Geomech. Abstr.*, **21** (1984) 339.
9. FABER, K. T. & EVANS, A. G., *Acta Metall.*, **31** (1983) 565-76.
10. OKADA, A. & HIROSAKI, N., *J. Mater. Sci.*, **25** (1990) 1656.
11. WOETTING, G., FEUER, H. & GUGEL, E., *MRS Symp. Proc.*, 287, Boston, MA, p. 146.
12. PETZOW, G. & HOFFMANN, M. J., *Mater. Sci. Forum*, **113-115** (1993) 91-102.
13. GAZZARA, C. P. & MESSIER, D. R., *Ceram. Bull.*, **56** (1977) 777-89.
14. WOETTING, G., KANKA, B. & ZIEGLER, G., *Non Oxide Technical and Engineering Ceramics*, ed. S. Hampshire. Elsevier Applied Science, London and New York, 1986, pp. 83-96.
15. KAWASHIMA, T., OKAMOTO, H., YAMAMOTO, H. & KITAMURA, A., *J. Ceram. Soc. Japan*, **99** (1991) 310-13.
16. KINGERY, W. D., *J. Am. Ceram. Soc.*, **46** (1963) 391-5.
17. LEE, D. D., KANG, S. L., PETZOW, G. & YOON, D. N., *J. Am. Ceram. Soc.*, **73** (1990) 767-9.
18. PROKESOVA, M. & PANEK, Z., *J. Mater. Sci.*, **25** (1990) 1709-13.
19. NAITO, N. & DE JONGHE, L. C., *J. Mater. Sci.*, **25** (1990) 1686-9.
20. MITOMO, M. & UENOSONO, S., *J. Mater. Sci.*, **25** (1991) 3940-4.
21. MIURA, M., IIDA, S. & IJIMA, H., *Ceramic Powder Science IV*, ed. S. Hirano & G. L. Messing. American Ceramic Society, Westerville, OH, 1991, pp. 669-74.
22. HERMEL, W., *Third Euro-Ceramics*, **3** (1993) 391-6.
23. TAJIMA, Y., *Mat. Res. Symp. Proc.*, **287** (1993) 189-97.
24. HIROSAKI, N., OKADA, A. & MATOBA, K., *J. Am. Ceram. Soc.*, **71** (1988) 144-7.
25. MEIBNER, E., KLEEBE, H. J. & ZIEGLER, G., *Third Euro-Ceramics*, **3** (1993) 397-403.
26. HOFFMANN, M. J. & PETZOW, G., *Mat. Res. Soc. Symp. Proc.*, **287** (1993) 3-15.
27. DRESSLER, W., Ph D Thesis, University of Stuttgart, 1993.
28. BECHER, P. F., LIN, H. T., HWANG, S. L., HOFFMANN, M. J. & CHEN, I-WEI, *Mat. Res. Soc. Symp. Proc.*, **287** (1993) 147-58.
29. MITOMO, M. & UENOSONO, S., *J. Am. Ceram. Soc.*, **73** (1990) 2441-5.
30. KOESSEL, W., *Naturw. Ges. Gottingen*, **2** (1927) 135-9.
31. KRAMER, M., HOFFMANN, M. J. & PETZOW, G., *J. Am. Ceram. Soc.* (submitted).